INL/CON-16-38078
PREPRINT

PHISICS/RELAP5-3D Results for Exercises II-1 and II-2 of the OECD/NEA MHTGR-350 Benchmark

International Congress on Advances in Nuclear Power Plants (ICAPP 2016)

Gerhard Strydom

March 2016

The INL is a
U.S. Department of Energy
National Laboratory
operated by
Battelle Energy Alliance

PHISICS/RELAP5-3D RESULTS FOR EXERCISES II-1 AND II-2 OF THE OECD/NEA MHTGR-350 BENCHMARK

Gerhard Strydom

Idaho National Laboratory (INL), 2525 N. Fremont Ave., Idaho Falls, Idaho, 83415, gerhard.strydom@inl.gov

The Idaho National Laboratory (INL) Advanced Reactor Technologies High-Temperature Gas-Cooled Reactor (HTGR) Methods group currently leads the Modular High-Temperature Gas-Cooled Reactor (MHTGR) 350 benchmark. The benchmark consists of a set of lattice-depletion, steady-state, and transient problems that can be used by HTGR simulation groups to assess the performance of their code suites.

This paper summarizes the results obtained for the first two transient exercises defined for Phase II of the benchmark. The Parallel and Highly Innovative Simulation for INL Code System (PHISICS), coupled with the INL system code Reactor Excursions and Leak Analysis Program (RELAP5-3D), was used to generate the results for the Depressurized Conduction Cooldown (DCC) (Exercise II-1a) and Pressurized Conduction Cooldown (PCC) (Exercise II-2) transients. These exercises require the time-dependent simulation of coupled neutronics and thermal-hydraulics phenomena, and utilize the steady-state solution previously obtained for Exercise I-3 of Phase I.

This paper also includes a comparison of the benchmark results obtained with a traditional system code "ring" model against a more detailed "block" model that include kinetics feedback on an individual block level and thermal feedbacks on a triangular sub-mesh. The higher spatial fidelity that can be obtained by the block model is illustrated with comparisons of the maximum fuel temperatures, especially in the case of natural convection conditions that dominate the DCC and PCC events. Differences up to 125 K (or 10%) were observed between the ring and block model predictions of the DCC transient, mostly due to the block model's capability of tracking individual block decay powers and more detailed helium flow distributions. In general, the block model only required DCC and PCC calculation times twice as long as the ring models, and it therefore seems that the additional development and calculation time required for the block model could be worth the gain that can be obtained in the spatial resolution and detailed data available for these transients.

I. INTRODUCTION

The MHTGR-350 benchmark has been sponsored by the Organization for Economic Cooperation and Development's (OECD's) Nuclear Energy Agency (NEA) since 2012. The technical specification is based on the 350-MW MHTGR design developed by General Atomics, with minor simplifications described in the benchmark specifications.[1,2] The HTGR methods group at INL is responsible for defining the specifications, leading the data-collection and comparison activities, and chairing the annual technical workshops. After the initial launch of the benchmark at the 2012 PHYSOR conference in Chicago, two more workshops were conducted in September 2013 (Paris, France) and December 2014 (Anaheim, United States). Various code-development and verification activities from participants in Germany, South Korea, and the United States are currently based on the MHTGR-350 benchmark, and summary papers and reports were published on the INL activities between 2012 and 2015.[3,4,5,6]

As part of the benchmark simulation activities, the PHISICS reactor physics package was coupled to the INL-developed system thermal analyses code RELAP5-3D to enable neutron transport calculations for the core, as well as more flexible cross-section handling in coupled core simulations.[6,7] The coupled PHISICS/RELAP5-3D code suite was used to generate the results for the first two transient exercises defined in Phase II of the benchmark: the DCC (Exercise II-1a) and PCC (Exercise II-2). The transients were all based on the steady-state solution previously obtained for Exercise I-3 of Phase I, as reported in Reference 5.

An overview of the scope and status of the MHTGR-350 benchmark is provided in Section II, and a short description of the PHISICS/RELAP5-3D capabilities and code architecture is included in Section III. The transient results obtained for the DCC and PCC events are presented in Sections IV and V, respectively.

II. OVERVIEW OF THE OECD/NEA MHTGR-350 BENCHMARK

The scope of the MHTGR-350 benchmark is to define a problem based on a common given data set, and to compare methods and tools in core simulation and thermal hydraulic analysis through a set of multi-dimensional computational test problems. The benchmark consists of three Phase I steady-state exercises, four Phase II transient exercises, and two Phase III lattice depletion exercises.

- **Phase I**
  - **Exercise I-1:** Neutronics-only steady-state solution for the 350-MW end-of-equilibrium-cycle MHTGR core using the provided geometry, material descriptions, and detailed cross-section libraries.[2]
  - **Exercise I-2:** Thermal-hydraulics-only steady-state core solution. Four sub-cases are defined, depending on the core bypass flow type and the use of fixed or variable thermo-physical material properties. A defined core power distribution map must be used, because no neutronics are involved in this exercise.
  - **Exercise I-3:** Coupled-neutronics thermal-hydraulic core steady-state solution. This exercise is a combination the first two exercises and the coupled steady-state solution must be calculated using the provided temperature-dependent cross-section library, burnup, and fluence distributions.
- **Phase II**
  - **Exercise II-1a/1b:** DCC transient with and without scram. Initial conditions for the transients are obtained from the steady-state solution of Phase I, Exercise 3.
  - **Exercise II-2:** PCC with scram to an equalization pressure of 5 MPa.
  - **Exercise II-3a/3b:** Water ingress with scram. Two variations of a multiple steam generator tube rupture accident are defined. In these transients, 125.4 kg of steam is injected into the primary system over 2 and 22 seconds, respectively.
  - **Exercise II-4:** Xenon stability test. Participants are expected to simulate a 100-80-100% power load follow transient that tracks the buildup and decay of xenon and the subsequent core reactivity behavior over 72 hours.

It is currently planned to finalize the simulation of the remaining transients (Exercises II-1b, II-3, and II-4) by the end of 2016. The radial core layout of MHTGR-350 design is shown in Figure 1, and the major core characteristics are summarized in **Error! Reference source not found.**. In Figure 1, the control rods (CRs), core barrel, and RPV are also indicated. A detailed description of the MHTGR-350 design can be found in the benchmark specification document which is available on request from the OECD/NEA.[2] The 1/3rd core numbering utilized for the benchmark data reporting and the discussion that follows in this paper is shown in Figure 2.

Table 1. MHTGR-350 main characteristics.

Description	Value
Power	350 MW(t)/165 MW(e)
Core/fuel design	Graphite moderated. 660 prismatic hex-blocks with 15.5 wt% enriched uranium carbide/oxide tristructural isotropic fuel compacts.
Coolant	Helium @ 6.39 MPa
Core inlet/outlet temperature	259/687°C

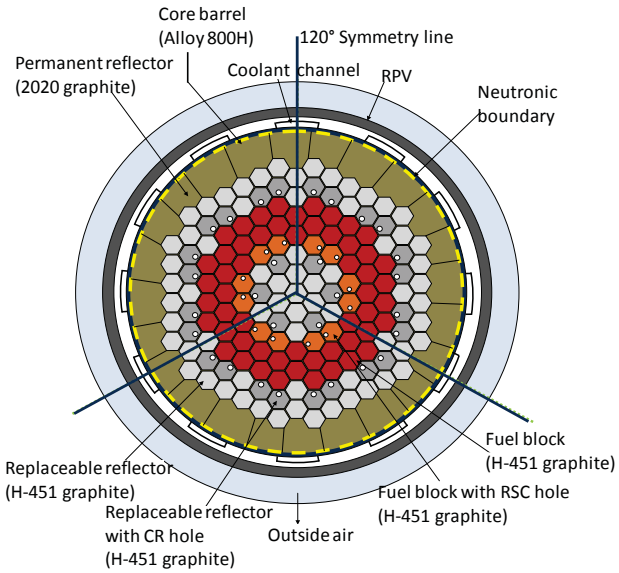

Figure 1. MHTGR-350 core radial layout.

III. PHISICS/RELAP5-3D CODE AND MODEL DESCRIPTIONS

III.A. PHISICS/RELAP5-3D Overview

The simulation of complex phenomena for advanced reactors, such as Generation IV systems, poses a challenge to existing thermal fluid system codes like RELAP5-3D.[7] For the analysis of the MHTGR-350 design, more advanced neutronic capabilities are required

compared to the available NESTLE neutronics package in RELAP5-3D, because the benchmark specifies the use of 26 energy groups (NESTLE is limited to four groups). During the development planning of the coupling of PHISICS to RELAP5-3D, it was decided to couple the different modules of PHISICS directly to RELAP5-3D (i.e., PHISICS is integrated in RELAP5-3D as a set of subroutines).

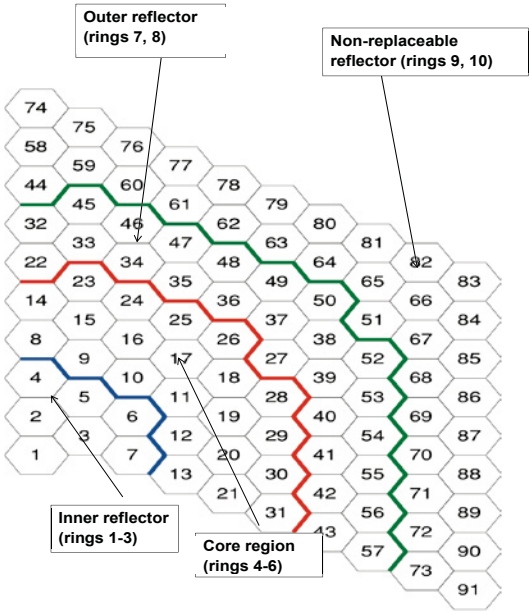

Figure 2. Core numbering layout (axial Layer 1).

PHISICS is a time-dependent neutronics code system developed at INL and consists of three modules: a nodal spherical harmonics transport core solver (INSTANT), a depletion module (Multi-Reactor Transmutation Analysis Utility [MRTAU]), and a cross-section mixer-interpolator (MIXER) module.[6] The INSTANT transport solver is parallelized and based on the second-order formulation of the transport equation discretized in angle by spherical harmonics. While in space, it uses orthonormal polynomials of an arbitrary order. A time-dependent scheme has been implemented in PHISICS, based on a second-order backward Euler scheme with explicit delayed neutron treatment.

MRTAU is a generic depletion code developed at INL that tracks the time evolution of the isotopic concentration of a given material. MRTAU utilizes a Taylor series expansion-based algorithm of arbitrary order and the Chebyshev rational approximation method for computation of the exponential matrix. This module is utilized to calculate the equilibrium xenon concentration for the steady-state condition and any dynamic xenon changes during transient events. The MIXER module performs all the cross-section handling for the different kernels. This module can treat macroscopic, microscopic, and "mixed" cross sections. More detailed descriptions of the PHISICS/RELAP5-3D coupling methodology can be found in Reference 6.

III.B. Ring and Block Model Descriptions

Two PHISICS/RELAP5-3D models were developed for the benchmark. The "ring" model followed the widely used system-code homogenization approach of modeling the inner reflector, fueled core region, and outer reflector as nine rings in cylindrical coordinates, with three additional rings representing the core barrel, RPV, and outer air boundary layer (Figure 3). Each of these rings is connected to its own heat structure representing fuel or graphite blocks on each axial level. The coarse axial mesh is discretized in two upper reflector, 10 core, and two lower reflector elements.

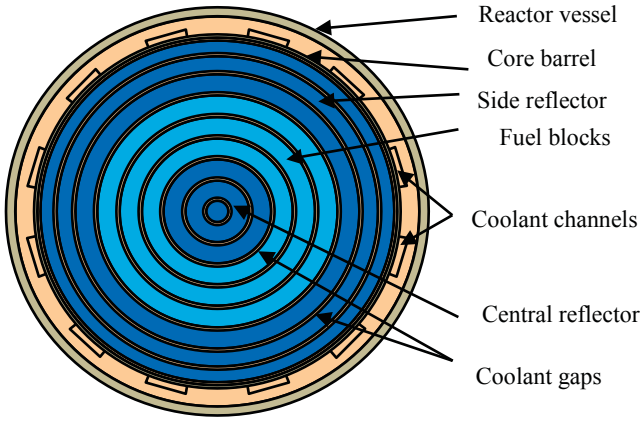

Figure 3. "Ring" model radial representation.

A number of conduction and radiation sets are included in the model to account for radial conduction and axial radiation between the graphite structures in the inner, outer, top, and bottom reflectors. Radial radiation heat transfer is also modeled between the outer reflector surface and the core barrel, and from the outer surface of the reactor vessel to the boundary air layer. Adiabatic boundary conditions are applied at the top and bottom model boundaries, and the outer radial air layer is defined to be at a constant temperature of 30°C.

A unit-cell approach is utilized for the three fuel rings to distinguish between the fuel and moderator temperatures. The cylindrical unit cell consists of a fuel compact, its surrounding matrix graphite and a helium coolant channel (Figure 4).

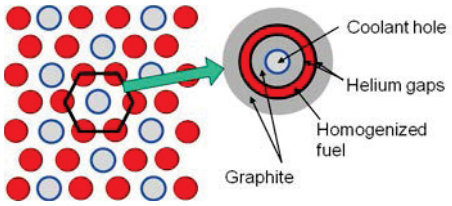

Figure 4. Unit-cell configuration.

This homogenized unit cell can be utilized in two spatial representations of the core geometry: the traditional "ring" model described above or a much more detailed "block" model. In the block model, a single hexagonal block can be explicitly represented by dividing it into six triangular elements, as shown in Figure 5. Each of the block faces can be connected to a RELAP5-3D pipe element that provides the helium mass flow rates, velocities, and temperatures along the axial height of the core. The corresponding triangular RELAP5-3D heat structure region connected to this pipe provides the heat source information in the case of the core fuel blocks.

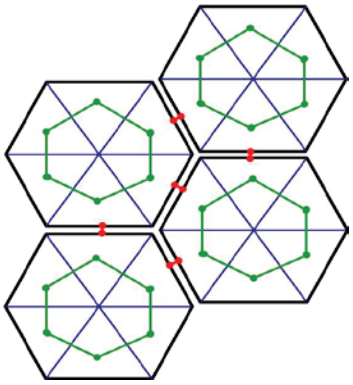

Figure 5. Block model conduction and radiation connections.

Heat transfer between the triangular elements occurs in two ways: inside a block via conduction and between blocks via radiation across the 2-mm gap between the block faces. These connections are defined as part of the conduction and radiation enclosure sets in the RELAP5-3D model, and corrections can be made for blocks that contain large CR or reserve shutdown holes. This "block" model can therefore provide a much more detailed temperature distribution compared to the ring model shown in Figure 3. In the case of the first fuel ring, for example, Blocks 8–13 in Figure 2 can now be represented with 6×6=36 triangular elements per axial layer, which provides 36 data points compared to only one value for the ring model.

For the steady-state thermal-hydraulics standalone Exercise I-2, a fixed power density was defined for each fuel block, but the modeling of coupled Exercise I-3 and the Phase II transients required the use of kinetic feedback zones to manage the exchange of power (calculated by INSTANT) and temperature (RELAP5-3D) data. There is, however, a limit on the number of these data types that the code can process. More detail on the input parameters utilized to create this model (e.g., material properties, decay heat profiles) can be found in the steady-state publications.[3,4]

A further RELAP5-3D restriction also requires that the left or right side of a heat structure can only be included in one type of enclosure (i.e., the left side of a triangular region cannot be connected to a conduction and radiation enclosure simultaneously). It was therefore decided to focus the RELAP5-3D triangular subdivision on the important regions of the active core region (Rings 4–6) and the two reflector rings next to the core (Rings 3 and 7). The RELAP5-3D block model (Figure 6) therefore consists of the "smeared-out ring" representation in Rings 1 and 2 (Blocks 1–3) and 8–10 (Blocks 44–91), and a detailed triangular resolution in Rings 3–7 (Blocks 8–43).

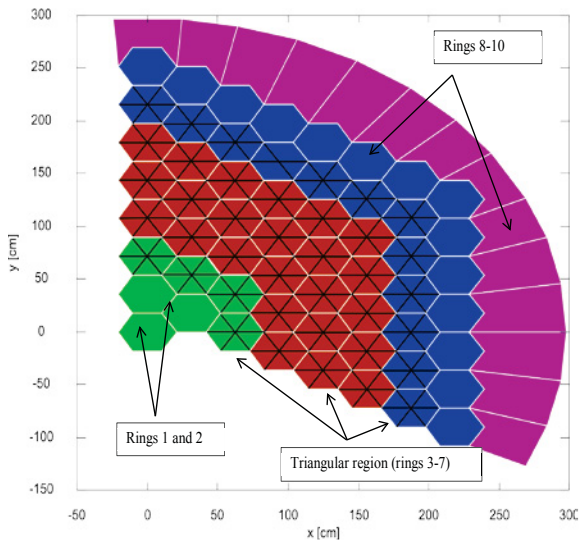

Figure 6. Ring and triangular geometry utilized in the block model.

Ring and triangular geometry utilized in the block model.

For the kinetic zone coupling between INSTANT and RELAP5-3D, it was initially envisaged to couple the triangular feedback elements on a one-to-one basis (i.e., one triangular node in RELAP5-3D would provide temperature data to a triangular node in INSTANT, which would then pass back the triangular power distribution to RELAP5-3D for the next iteration). Because the modeling of the full MHTGR-350 core graphite structures in a triangular geometry requires 7,644 kinetic nodes

(91 blocks on 14 layers with six triangles each), a full core triangular model was not an option due the limitations in the number of kinetic zones available in RELAP5-3D.

On the neutronics side of the coupling, INSTANT uses a hexagonal mesh for the neutronics solution corresponding to a fuel or reflector block, corresponding to a single flux or power value per block.

IV. EXERCISE II-1A RESULTS: DCC WITH REACTOR TRIP

The results obtained with the PHISICS/RELAP5-3D ring and block models for DCC event are presented in this section. The focus is here on the maximum fuel temperatures and power variations as functions of time, because these parameters are the main figures of merit during these accident sequences. (The event sequences specified here should not be seen as representative of the MHTGR safety case but purely as the basis for code-to-code comparisons.)

The DCC event is the equivalent of a loss-of-cooling accident in light-water reactors and represents the bounding case for the fuel temperatures. It is usually initiated by a break in the system pressure boundary. The transient was simulated for a period of 100 hours after the pressure boundary break, using the boundary conditions indicated in the benchmark specification[2]:

- A reactor trip is performed after 30 seconds by inserting all CRs. The provided decay heat fit for each individual block was used for this exercise.
- The system pressure equalized at atmospheric (100 kPa), and the inlet mass flow rate decreased to 0 kg/second. It is assumed that the decrease in the pressure and mass flow rates are linear between 0 and 20 seconds.
- The restart file created for Phase I Exercise I-3a was used as the starting point for the DCC simulation. Exercise I-3a was a steady-state solution utilizing the specified 11% bypass flow distribution and variable thermo-physical properties (TPs).
- The effects of non-local heat deposition (e.g., outside the fuel kernels via fast neutrons and gammas) were neglected.

Because the coupled PHISICS/RELAP5-3D simulations typically take twice as long to complete as the standalone cases, only the steady state created in Exercise I-3a is used for the coupled DCC calculation. However, it is interesting to assess the effect on the DCC when different steady states are used as starting points. The fixed-power restart points created for Exercises I-2a, I-2b, and I-2d are used here as input for the RELAP5-3D standalone calculations. These four thermal-fluid-only cases were defined as follows:

- Exercise I-2a: No core bypass flows are simulated, and fixed TPs are used.
- Exercise I-2b: A total of 11% core bypass flow distribution is implemented with fixed TPs.
- Exercise I-2c: The 11% core bypass flow distribution is combined with TPs that depend on fluence and temperature.
- Exercise I-2d: The bypass flows were obtained by explicitly solving the flow through the 2-mm gaps between the fuel and reflector blocks, and the flows were combined with variable TPs.

The axial power shape in fuel Ring 1 is shown in Figure 7 for the two model types discussed here: (1) the fixed/specified power distribution provided for the RELAP5-3D standalone Cases I-2 and (2) the fully coupled PHISICS/RELAP5-3D Case I-3 where the fission power profile needs to be calculated. The axial power distributions are both peaked at the top of the MHTGR core due to the colder temperatures and the fuel nuclide inventory, but the PHISICS power peaking factor is higher than the fixed model case due to the feedback effects from the fuel, moderator temperature, and equilibrium xenon concentration.

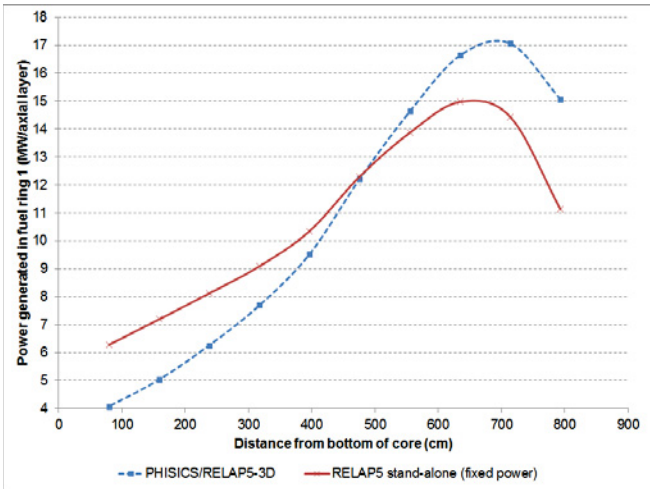

Figure 7. Comparison of power generation (MW) per axial level in fuel Ring 1 between the fixed-power and PHISICS ring models.

The maximum fuel temperatures reached during the DCC transient are shown in Figure 8 for the ring and block models. The data set shown here was created with RELAP5-3D using fixed-power inputs and the steady states created in Phase I for Exercises I-2a through I-2d. It

can be seen that the block models consistently predict significantly higher fuel temperatures compared to the corresponding ring models, and also that the block model peak values occur earlier into the transient.

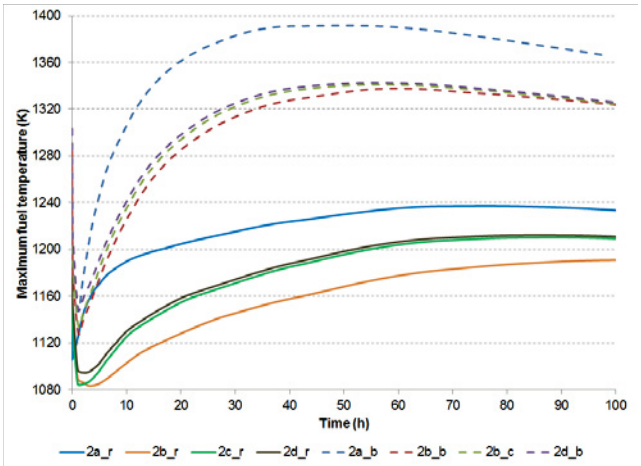

Figure 8. Comparison of DCC maximum fuel temperature (K) vs. time for the ring and block models, based on fixed-power versions of Exercises I-2a through I-2d.

For Exercise 2a (no bypass flows), the block model peak value of 1,391 K is reached at 50 hours, while the ring model peak of 1,237 K is delayed until 74 hours after the start of the break. As was stressed during the discussion of the steady-state results,[5] it should be noted that without experimental data that can be used for validation purposes, it is difficult to conclude which of the two models are providing a more accurate prediction of the fuel temperature behavior. However, because the ring model homogenizes large volumes of the fuel and reflector regions, it can be expected that local hot spots will not be adequately represented by this approach.

For the block model, the spread between the Exercise I-2b, I-2c, and I-2d results is very small, indicating the effect of including the bypass flows in the reflector regions. The use of fixed or variable TPs does not result in significant differences. The ring model for Ex. I-2b does, however, predict temperatures that are approximately 20 K lower than those in Exercises I-2c and I-2d, which again illustrates the difference in spatial resolution between the ring and block models.

The coupled PHISICS/RELAP5-3D DCC calculation uses as a starting point that the steady-state restart file created at the end of Exercise I-3a.[5] This model is based on the RELAP5-3D model developed for Exercise I-2c. The DCC fuel temperatures obtained by using both of these models (PHISICS coupled and RELAP5-3D fixed-power) are compared in Figure 9.

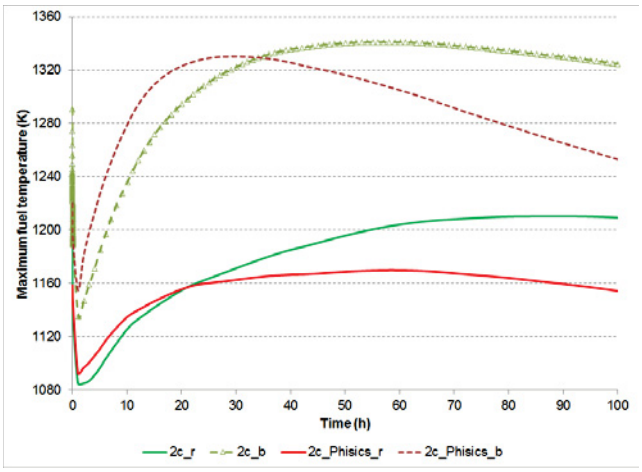

Figure 9. Comparison of DCC maximum fuel temperature (K) vs. time for the ring and block models based on fixed-power versions of Exercise I-2c and the PHISICS/RELAP5-3D data for Exercise II-1a.

As noted previously, the block models for both PHISICS and the fixed-power variants predict significantly higher fuel temperatures than the ring model values. However, both the ring and block versions of the PHISICS model peak earlier and at lower temperatures than the fixed-power cases, although the differences are relatively small (i.e., less than 50 K, or 5%, for most of the transient duration). These differences can primarily be ascribed to variances in the fuel and reflector temperatures between these models during the steady-state and early stages of the DCC.

The RELAP5-3D temperature block model consists of six triangular cells, but due to the limitations on the model size, the power feedback is based on the block level (i.e., each triangle receives the same homogenized power density from PHISICS). During the DCC transient, the initial differences that exist within the block elements (Figure 10) reduce to zero, because the decay power feedback assigns the same power density to each triangle and the forced helium flow terminates. It is therefore sufficient to compare the change in the various block temperatures over the duration of the DCC event.

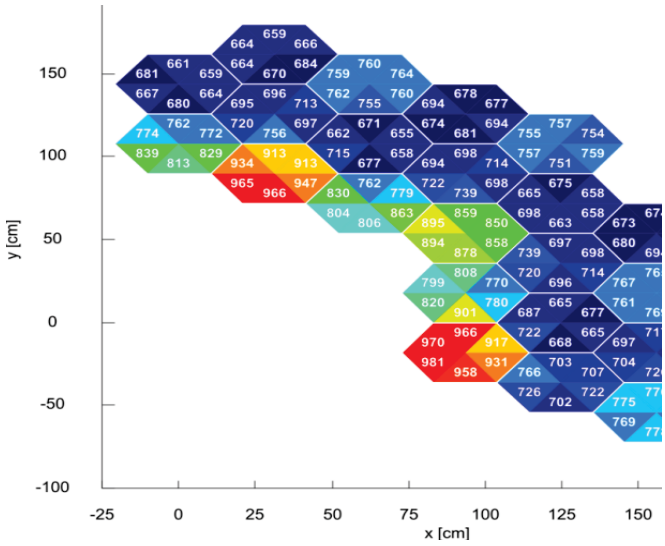

Figure 10. Exercise I-2a – Average fuel temperature (°C) distribution on axial level 1 (first bottom core level) for the block model during steady state.[5]

The changes in maximum fuel temperature for the six inner fuel blocks in Fuel Ring 1 are shown in Figure 11 for the coupled PHISICS/RELAP5-3D model based on Exercise I-2c. The difference between the coldest (11) and hottest (8) block is less than 30 K (or 2.5%) for most of the transient. The different heat-up trajectories of the six blocks are also shown, with Block 9 initially reaching the lowest temperature within the first 2 hours.

After approximately 10 hours, the lowest temperature is produced by Block 11, because it has the lowest decay heat assigned to it (see Figure 12).

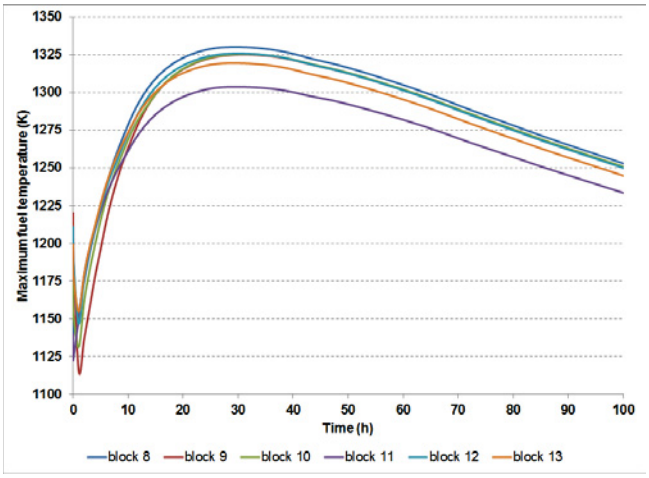

Figure 11. Comparison of DCC maximum fuel temperature (K) vs. time for Blocks 8–13 based on PHISICS/RELAP5-3D data for Exercise II-1a.

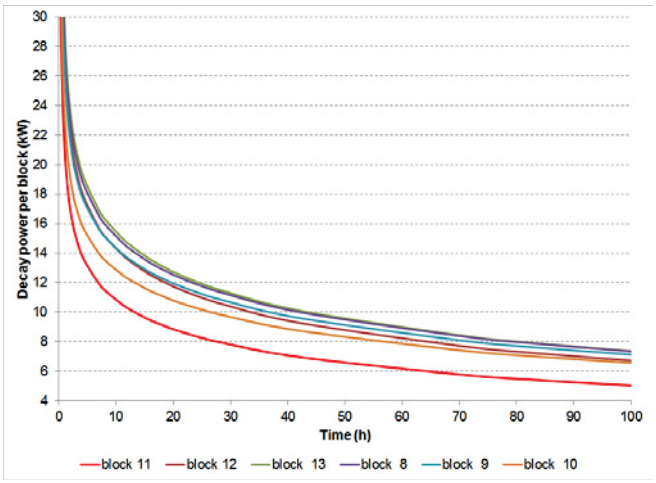

Figure 12. Comparison of decay heat (kW) generated by Blocks 8–13.

V. EXERCISE II-2 RESULTS: PCC WITH REACTOR TRIP

The PCC event is also referred to as a pressurized loss-of-forced-cooling accident and can be initiated by a turbine trip. No pressure boundary break occurs during this transient, and it is significantly more probable than the DCC event. An approach similar to that discussed in Section IV for the DCC is followed here for the analysis of the PCC event. Additional assumptions and boundary conditions are as follows:

- The turbine spin-down is assumed to be completed at 30 seconds. The CRs are inserted (reactor trip) to the shutdown position 60 seconds into the transient.
- The effects of natural convection were calculated for this exercise, because the full helium coolant inventory is still present in the primary system. During the first few minutes, the system pressure equalizes at the stagnant system pressure of 5 MPa when the turbines have completed the spin-down phase, and the inlet mass flow rate decreases to 0 kg/second. The pressure was kept constant at 5 MPa for the duration of the transient.

A comparison of the maximum fuel temperature over the first 100 hours of the PCC event is presented in Figure 13 for the ring and block RELAP5-3D models. The data set shown here was created with RELAP5-3D using fixed-power inputs and the steady states created in Phase I for Exercises I-2a, I-2b, and I-2d. Coupling with PHISICS was therefore not required for these cases. The ring and block models exhibit similar variations with time, with the block models consistently predicting fuel temperatures that peak earlier and higher than the ring models.

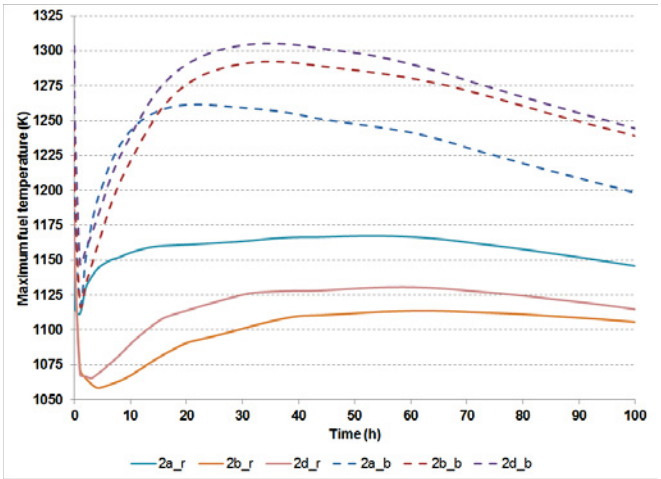

Figure 13. Comparison of PCC maximum fuel temperature (K) vs. time for ring (r) and block (b) models based on fixed-power versions of Exercises I-2a, I-2b, and I-2d.

The Exercise I-2a models (no bypass flow, fixed TP properties) both peak earlier than the Exercise I-2b and I-2d models that simulate the hotter core and colder reflectors. The variation between the models are, however, relatively small (generally less than 50 K or 4%), but the differences between the block and ring models are significant (up to 180 K or 16% at some time points).

The results obtained for the PCC based on Ex. I-2c, as well as the coupled PHISICS/RELAP5-3D results for Exercise II-2, are shown in Figure 14. In general, the trends observed for the PCC event are similar to those in the DCC data set but with all PCC fuel temperatures significantly lower due to the increased natural convention at 5 MPa. This is especially apparent for the block model PCC case, which is up to 120 K colder than the DCC block model case, as shown in Figure 14. The rise in maximum fuel temperature is also much flatter over time, because the enhanced convection distributes heat from the hot regions of the core much more effectively than in the DCC case. It is interesting to note that the ring model predicts a smaller difference of less than 50 K between the PCC and DCC transients, because this model cannot distinguish between variations in block decay heat generation and natural convection effects on a finer spatial scale. From the data shown in Figure 14, the block model therefore seems to be especially valuable for simulating the atmospheric pressure DCC case in more detail, where the very low mass flow rates are notoriously difficult to solve accurately.

The importance of the reflector temperatures during these PCC events is illustrated by the temperature distribution shown in Figure 15.

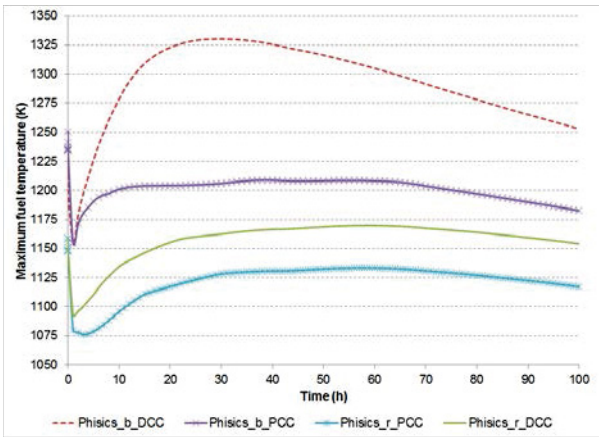

Figure 14. Comparison of PCC and DCC maximum fuel temperature (K) vs. time for ring (r) and block (b) models based on PHISICS/RELAP5-3D versions of Exercise I-2c.

In the absence of convective cooling, the only heat-removal mechanism for the decay heat stored in the fuel region is through conduction and radiation in the side reflector graphite and the vessel. Because the reflector structures are significantly colder due to bypass flows for Exercises I-2b and I-2d (up to 48% in some locations), heat transported to the radial boundary at the RV is absorbed here, resulting in lower peak fuel temperatures over time. In contrast to this, the reflector temperatures for Exercise I-2a are relatively high (no bypass flows), which results in a delay in the flow of energy outward from the fuel to the RV due to a much flatter temperature gradient.

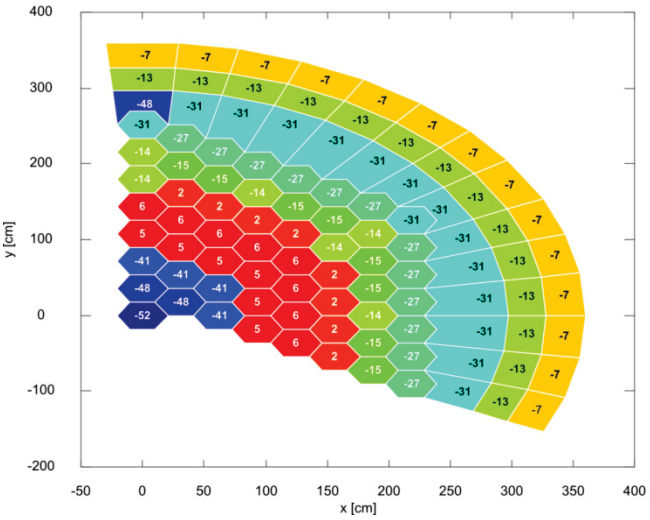

Figure 15. Average graphite temperature difference (%) between Exercises I-2a and I-2b for all graphite structures in the ring model on axial Level 1 (first bottom core level).[5]

During the PCC, heat is transported from the hot bottom region of the core to the colder upper region via natural convection flows (at very low rates, typically less than 0.5 kg/second). Over time, the fuel temperatures will reflect the decay heat production distribution shape in the absence of the dominating effect of forced downward flow. The change in the axial profile of the inner fuel ring fuel temperature is shown in Figure 16 for six time points during the PCC: at steady state and then at 35 seconds, 1 hour, 10 hours, 35 hours, and 100 hours into the transient.

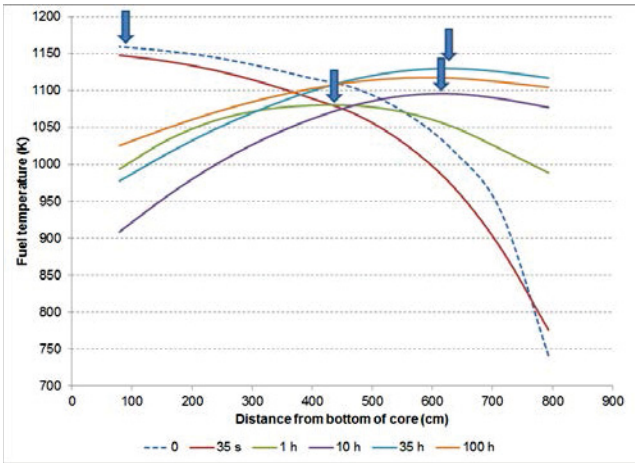

Figure 16. Change in fuel Ring 1 axial fuel temperature (K) profile at six time points during the PCC event.

The blue arrows indicate how the peak values change over time: at t = 0 seconds, the highest fuel temperature is reached at the core outlet due to the forced convection, while after only 35 seconds into the PCC, the redistribution of heat has already reached the upper regions of the core. Within the first hour, a significantly flatter profile is visible, with the upper core region now at the same temperature as the bottom of the core. After 10 hours, the process is almost complete, and the dominant axial distribution can be seen exhibiting a peak around 650–700 cm from the bottom of the core. This profile is caused by the generation of fission product decay heat in the typically top-peaked MHTGR-350 core (as shown in Figure 7).

VI. CONCLUSIONS

This paper summarized the INL results obtained for the DCC (Exercise II-1a) and PCC (Exercise II-2) transients defined for Phase II of the OECD MHTGR-350 benchmark. The transients were simulated using both the fixed-power RELAP5-3D standalone models generated for Exercise I-2, as well as the coupled PHISICS/RELAP5-3D model created for Exercise I-3.

The results were compared using two modeling approaches: a traditional system code ring model and a much more detailed block model that include kinetics feedback from individual blocks and thermal feedbacks on a triangular sub-mesh. The higher fidelity that can be obtained by the block model was illustrated with comparisons of the maximum fuel temperatures, especially in the case of low mass flow conditions that dominate the DCC and PCC events. Differences up to 125 K (or 10%) were observed between the ring and block model predictions of the DCC transient, mostly due to the block model's capability of tracking individual block decay powers and much more detailed natural convection helium flow distributions.

In general, the block model only required DCC and PCC calculation times twice as long as the ring models. Therefore, it seems that the additional development and calculation time required for the block model is worth the gain obtained in spatial resolution and detailed data available for these transients, but also that the relative performance of the ring model is still suitable for scoping calculations. Without actual experimental validation, it cannot be concluded that the block model represents a more accurate or "correct" model compared to the ring model, but the gain in spatial information is a significant advantage. The difference between the results of the four sub-cases was mostly minimal, but larger variances were observed when the bypass flows were included in the models.

The MHTGR-350 benchmark provides a challenging simulation set of problems, even with the simplifications introduced in the benchmark specification. This activity represents an important contribution to the code-to-code verification of modern prismatic HTGR codes. The third and final benchmark workshop is currently planned for May 2016, and it is expected that the final comparison report of the Phase I (steady-state) and Phase III (lattice-depletion) results for all participants will be released by the OECD/NEA toward the end of 2016.

ACKNOWLEDGMENTS

This work was supported by the U.S. Department of Energy, Assistant Secretary for the Office of Nuclear Energy, under DOE Idaho Operations Office Contract DE-AC07-05ID14517.

The author wishes to acknowledge the significant contributions made to the benchmark results by his INL colleagues Aaron Epiney (developer of the original PHISICS/RELAP5-3D model and code coupling in 2011) and Andrea Alfonsi for the numerous code improvements and developments implemented since 2013.

REFERENCES

1. J. ORTENSI, et al., “Prismatic Core Coupled Transient Benchmark,” *Trans. of the American Nuclear Society,* **104**, p. 854 (2011).
2. J. ORTENSI, et al., “Prismatic Coupled Neutronics/Thermal Fluids Transient Benchmark of the MHTGR-350 Core Design: Benchmark Definition,” Draft, Organization for Economic Corporation and Development (2014).
3. A. EPINEY, et al., “New Multi-group Transport Neutronics (PHISICS) Capabilities for RELAP5-3D and its Application to Phase I of the OECD/NEA MHTGR-350 MW Benchmark,” *Proc. of conf. HTR 2012,* Tokyo, Japan (2012).
4. G. STRYDOM, et al., “INL Results for Phases I and III of the OECD/NEA MHTGR-350 Benchmark,” INL/EXT-13-30176, Idaho National Laboratory (2013).
5. G. STRYDOM, et al., “Comparison of the PHISICS/RELAP5-3D Ring and Block Model Results for Phase I of the OECD MHTGR-350 Benchmark,” *Nuclear Technology*, in publication (2016).
6. C. RABITI, A. ALFONSI, A. EPINEY, “New Simulation Schemes and Capabilities for the PHISICS/RELAP5-3D Coupled Suite,” *Nuclear Science and Engineering*, Vol. 182, No. 1 (2016).
7. RELAP5-3D© Code Manual, Vol.1-5, Rev. 3, INEEL-EXT-98-00834, Idaho National Laboratory (2009).